Nanoscale

ROYAL SOCIETY OF CHEMISTRY

COMMUNICATION

View Article Online
View Journal | View Issue

Cite this: *Nanoscale*, 2025, **17**, 7753

Received 12th December 2024,
Accepted 20th February 2025

DOI: 10.1039/d4nr05253f

rsc.li/nanoscale

FRET-driven hybrid polymer–perovskite matrices for efficient pure-red emission†

Jyoti Saxena,*[a] Rahul Murali,[b] Avari Roy,[a] Abdullah A. Al-Kahtani,[c] Venugopal Rao Soma,[d,e] Sai Santosh Kumar Raavi[b] and Aditya Sadhanala*[a,c]

Achieving efficient pure-red emission in perovskite-based high-definition display applications remains challenging due to persistent spectral, thermodynamic, and operational instability. Although significant progress has been made using red-emitting quasi-2D perovskites, quantum dots, and mixed-halide perovskites, their performance under operational conditions often remains limited. Here, we address these challenges by embedding mixed-halide perovskite nanocrystals (PeNCs) into a polymer matrix to create a donor–acceptor architecture. This hybrid system stabilizes the nanocrystals and enables efficient energy transfer *via* Förster resonance energy transfer (FRET). We observe enhanced acceptor photoluminescence and reduced donor lifetimes, confirming the effective FRET-mediated energy transfer arising from optimal spectral overlap. With a FRET rate of 0.18 ps^{-1} and a FRET efficiency of 88.9%, our approach provides spectrally stable, enhanced pure-red emission. Moreover, it demonstrates a pathway for designing customized energy cascades, paving the way for next-generation optoelectronic devices with improved stability and performance.

[a]*Centre for Nano Science and Engineering, Indian Institute of Science, Bengaluru 560012, Karnataka, India. E-mail: jyotiphysics06@gmail.com, sadhanala@iisc.ac.in*
[b]*Ultrafast Photophysics and Photonics Laboratory, Department of Physics, Indian Institute of Technology Hyderabad, Kandi 502285, Telangana, India*
[c]*King Saud University, College of Science, Chemistry Department, P. O. Box 2455, Riyadh-11451, Saudi Arabia*
[d]*School of Physics, University of Hyderabad, Hyderabad 500046, Telangana, India*
[e]*DRDO Industry Academia – Centre of Excellence (DIA-CoE; formerly ACRHEM), University of Hyderabad, Hyderabad 500046, Telangana, India*
†Electronic supplementary information (ESI) available. See DOI: **https://doi.org/10.1039/d4nr05253f**

Aditya Sadhanala

Dr Aditya Sadhanala is a distinguished researcher at the Indian Institute of Science, specializing in nanoscience and optoelectronics. Recipient of multiple international awards for his groundbreaking work in nanomaterials and device engineering, Dr Sadhanala is dedicated to translating cutting-edge research into societal benefits through strategic industry collaborations. His innovative projects advance sustainable energy and smart technologies, addressing critical global challenges. Beyond his research, he is actively involved in outreach efforts, including public lectures, science communication initiatives, and community workshops to promote scientific literacy. Passionate about societal impact, he partners with global industry leaders to develop practical solutions and mentors the next generation of scientists. Dr Sadhanala's commitment bridges fundamental science, industrial applications, and societal needs, fostering technological innovation and broader community engagement.

Metal halide perovskites have emerged as one of the most promising semiconducting materials in the field of optoelectronics, especially for light-emitting diodes (LEDs), owing to their outstanding properties, such as high photoluminescence quantum yield (PLQY), exceptional color purity with narrow full-width-at-half-maximum (FWHM), wide color gamut, low manufacturing costs, and the ability to tune their emission spectrum.[1] Efficient pure-red emission (620–650 nm)[2] is critical for high-definition display applications and is a fundamental requirement for compliance with the Rec. 2020 standard, which defines the color gamut for advanced display technologies.[3]

Several strategies have been explored to achieve efficient red emission using metal halide perovskites. One extensively studied approach involves exploiting the quantum confinement effect[4,5] by minimizing the size of perovskite nanocrystals close to their Bohr radius.[6] However, this involves severely downsizing the PeNCs[7] leading to significant thermodynamic instability,[8] and compromises both optical and electrical performance.[9] Alternatively, pure iodide-based quasi-2D perovs-

kites with self-assembled multiple quantum wells (different *n*-phases) have demonstrated potential for pure red emission.[10–12] However, the spontaneous formation of various *n*-phases in quasi-2D perovskite films can result in undesirable phase distribution,[13] affecting spectral purity.[14] Mixed-halide (bromide-iodide) PeNCs provide a relatively straightforward route for spectral tuning toward red emission,[15] but issues such as halide segregation and long-term instability persist.[16,17] Given these challenges, it is important to develop alternative pathways to obtain efficient red emission required for the development of high-performance displays.

Incorporating PeNCs into polymer matrices presents a promising strategy to enhance perovskite emission properties. Specifically, FRET can be leveraged within polymer–PeNC composites to boost photoluminescence (PL) efficiency and achieve enhanced red emission. While polymer–perovskite composites have been extensively studied,[18–20] the potential of FRET-driven red luminescence enhancement in such systems remains unexplored. Addressing this gap could provide new insights into enhancing emission, simplifying fabrication processes, and advancing the development of high-performance red-emitting perovskite LEDs (PeLEDs).

Exploiting energy or charge transfer mechanisms in electronically active polymer blends has been a prevalent strategy to enhance the performance of organic light-emitting diodes (OLEDs).[21–23] Various polymer–polymer, polymer–small molecule, and polymer–inorganic complex blends have been employed to achieve efficient energy transfer through the FRET mechanism.[24] In this process, a photoexcited high-energy gap host material (donor) interacts with a neighbouring ground-state low-energy gap guest material (acceptor) by transferring excitation energy.[25–28] Effective FRET in blended systems requires significant spectral overlap between the host emission and guest absorption spectra,[29–31] along with uniform dispersion of both materials.[29] This energy transfer process prevents self-absorption losses and reduces concentration quenching of generated excitons, thereby improving overall emission efficiency.[31–33]

In this work, we demonstrate a polymer–PeNC blend system that enables highly efficient FRET, resulting in enhanced pure-red emission. By employing methylammonium-based lead mixed-halide PeNCs ($MAPbI_2Br$) as the emissive guest material within a polymer matrix, we achieve significant photoluminescence enhancement using a relatively simple and scalable approach. The PeNCs are incorporated into the hole-transporting materials, poly (9,9-dioctylfluorene-*co*-*N*-(4-butylphenyl)diphenylamine) (TFB) and 4,4′-bis (*N*-carbazolyl)-1,1′-biphenyl (CBP), which together serve as the host in the perovskite–polymer blend system. The ternary blend of PeNCs, TFB, and CBP facilitate both cascade energy and charge transfer. All three components exhibit good miscibility, and the significant spectral overlap between the emission spectrum of the donor (TFB) and the absorption spectrum of the acceptor (PeNCs) enables efficient nonradiative energy transfer from TFB to PeNCs when excited at the absorption peak wavelength of TFB. To the best of our knowledge, this is the first demonstration of using a polymer–PeNCs composite for obtaining enhanced red emission *via* FRET. Our findings through this study highlight the potential of FRET-driven emission enhancement in perovskite–polymer composites, offering a viable pathway toward the development of high-performance red-emitting PeLEDs.

The molecular structures of TFB[34] and CBP[34] are shown in Fig. 1(a and b), and the flat-band energy levels of $MAPbI_2Br$ PeNCs, CBP,[35] and TFB[35] are depicted in Fig. 1c. The UV-Vis spectrum of PeNCs and PL spectrum of TFB in the solid films are shown in Fig. 1d. There is a significant overlap between the emission spectrum of the TFB and the absorption spectrum of the PeNCs in the region from 421 nm to 478 nm. This is an essential prerequisite for realizing a donor–acceptor energy-transfer system. According to this spectral alignment, the TFB appears suitable as a donor, while the PeNCs can accept energy from the donor system.

The UV-Vis spectrum of the ternary blend of CBP, TFB, and PeNCs was obtained, illustrating that it bears a strong resemblance to the combined spectral features of its individual components, albeit with slight deviations from an ideal linear superposition (Fig. 1e). The retention of distinct spectral features implies that the mixing process does not significantly perturb their individual identities. The monodispersity of the PeNCs is indicated by transmission electron microscope (TEM) image in Fig. 2b. A homogeneous polymer–PeNCs blend without any phase separation is crucial for enhanced energy-transfer and long-term stability of the film, atomic force microscope (AFM) image of the CBP–TFB–PeNCs blend film supports the formation of homogeneous surface morphology with no visible phase separation (Fig. 2c).

To investigate possible energy-transfer processes between TFB and PeNCs, we prepared a 1 : 1 volume ratio mixture of CBP and TFB solutions and added a PeNC dispersion to this solution in fixed volume ratios. Thus, we obtained the following ratios (CBP + TFB) : PeNCs-1 : 3, 1 : 5, and 1 : 8. Solid-state films were prepared by spin-coating these mixtures onto glass substrates, and the PL emission spectra of the films were acquired (Fig. 2a). The films of all blends were optically excited at 400 nm to create a population of excited TFB molecules. In this wavelength region, direct absorption by CBP or PeNCs is negligible. The resulting PL emission spectrum is stable and is a blend of direct luminescence from the excited TFB and luminescence from the PeNCs. In addition, the PL emission of the donor decreased, whereas that of the acceptor increased for all the blends. This corresponds to energy transfer in these blends as donor-emitted photons are reabsorbed by the acceptor through the Förster mechanism.[36]

To further confirm the energy-transfer processes, we employed a femtosecond transient absorption spectroscopy (fs-TAS) setup to investigate the lifetimes of the donor in the pristine and blended films, and to investigate the time scales at which these energy-transfer processes occur from donor to acceptor in the solid-state heterostructures. TA spectroscopy is a powerful technique for investigating excited-state dynamics. The samples were excited using a pump beam with a wavelength of 400 nm, and a white light continuum (450–780 nm)

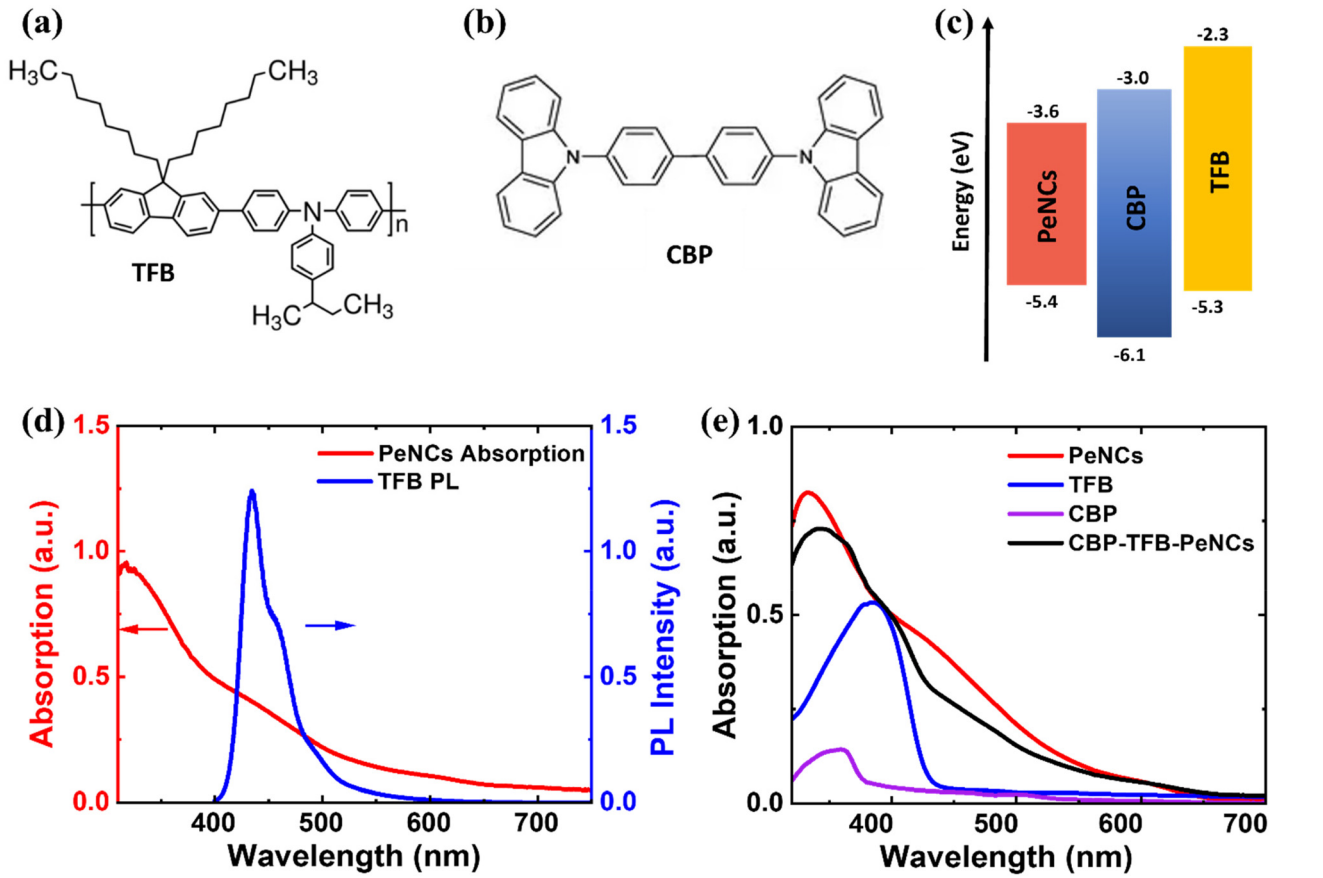

Fig. 1 (a) Molecular structure of TFB,[34](b) Molecular structure of CBP,[34] (c) Flat-band energy levels of $MAPbI_2Br$ PeNCs, CBP,[35] and TFB,[35] (d) Spectral overlap between absorption spectrum of PeNCs (red line) and PL spectrum of TFB (blue line), and (e) UV-Vis spectra of the PeNCs, CBP, TFB, and their blend (CBP–TFB–PeNCs).

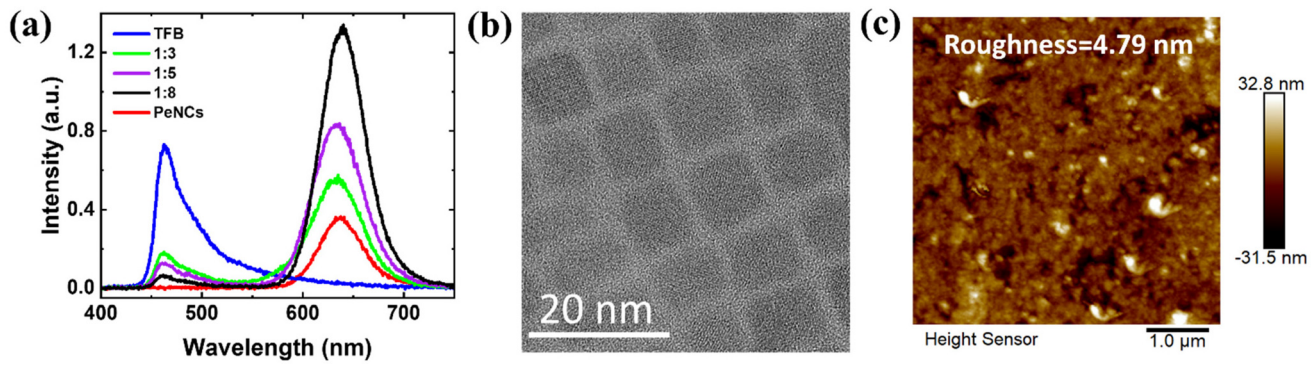

Fig. 2 (a) Energy transfer between TFB and PeNCs in thin films. PL spectra of thin films of TFB, PeNCs and blends of CBP–TFB–PeNCs in different ratios, (b) TEM image of PeNCs, and (c) AFM image of the CBP–TFB–PeNCs blend.

was used to probe the excited-state dynamics of the system. The fs-TA spectra for all the samples with increasing delay times for TFB, PeNCs, and (CBP + TFB) : PeNCs (1 : 3, 1 : 5, and 1 : 8) are shown in Fig. 3(a–e). Various spectral features were observed for different wavelength regimes. For the donor TFB, we observed two spectral signatures: (i) a negative signal, corresponding to the ground state bleach (GSB) and the stimulated emission in the initial wavelength regime, followed by (ii) a longer-lived positive signal, photoinduced absorption (PIA) in the 510–780 nm regime. Pristine PeNCs exhibited a positive signal in the range 450–520 nm, followed by a negative signal ranging from 520–640 nm, which can be assigned to the ground state bleach, which is attributed to the state filling effect. A red shift in the GSB is observed with time, which can

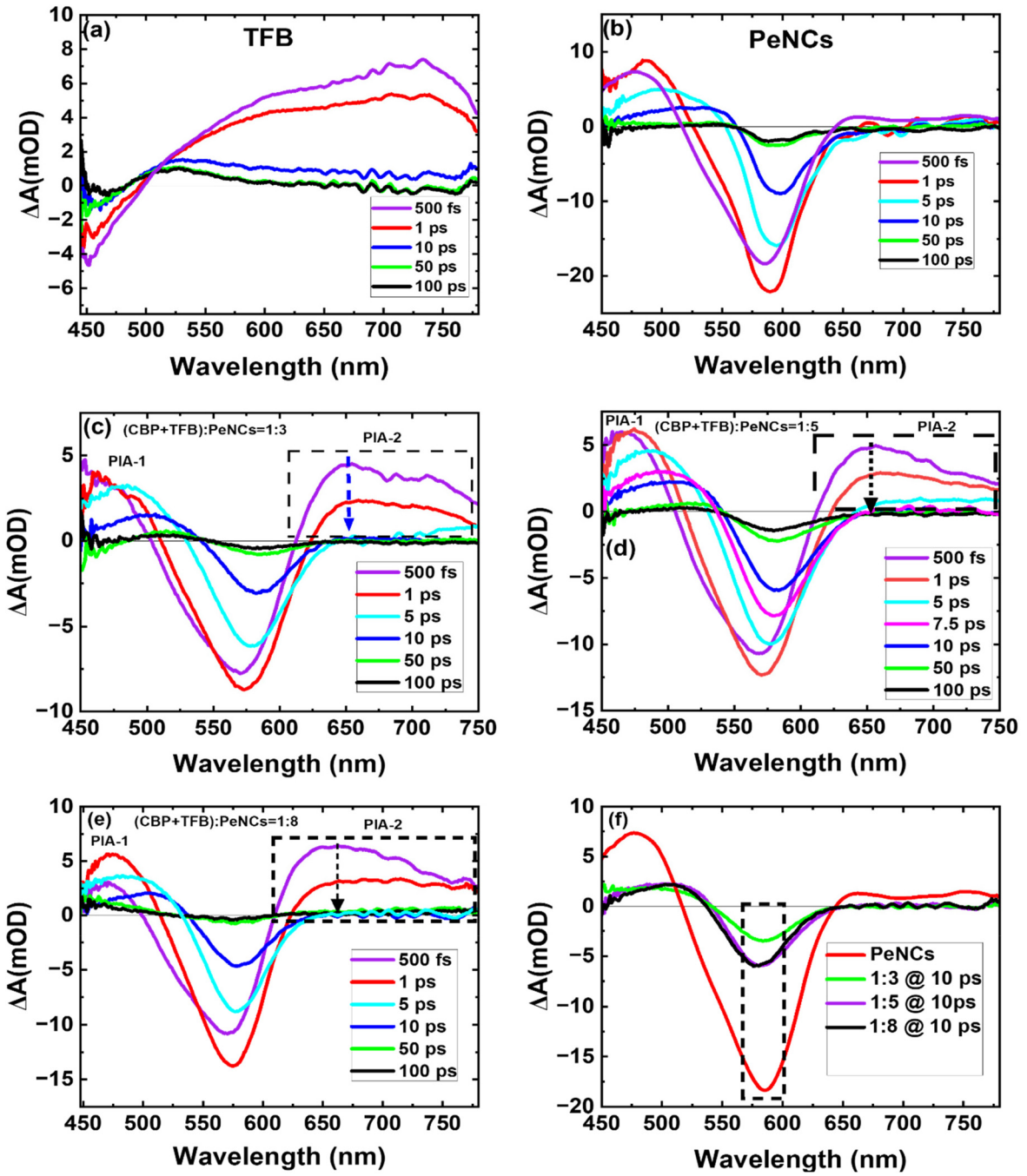

Fig. 3 Femtosecond TA spectral evolution for (a) TFB, (b) PeNCs, (c) (CBP + TFB) : PeNCs (1 : 3), (d) (CBP + TFB) : PeNCs (1 : 5); (e) (CBP + TFB) : PeNCs (1 : 8), and (f) Wavelength spectra of all the blends (1 : 3, 1 : 5, 1 : 8) and pristine PeNCs following a similar spectra with a common peak around 580 ps.

be assigned to bandgap renormalization.[37] Another positive signal (PIA-2) centered at approximately 650 nm appeared in the initial timescales following photoexcitation. Within 1 ps, this PIA-2 rapidly shifted into the GSB owing to carrier cooling.[38] However, for the blend films, it is evident from the spectra that the blends exhibit spectral features of both the donor and the acceptor. The positive signals (PIA-1) and bleach (GSB-1) observed in the blends correspond to that of PeNCs, whereas the second positive signal observed after 620 nm indicates the signature of TFB.

Among the blends, the 1 : 5 and 1 : 8 ratios, with a higher acceptor concentration, exhibited more intense bleach and PIA-1 corresponding to the PeNCs. Initially, after photoexcitation, we observed contributions from both TFB and PeNCs in the PIA-2 region. As the probe delay increases, the PIA-2 observed in all three blends, as well as in the TFB, was

reduced. However, the TAS spectra of the blends (Fig. 3(c–e)) indicate that PIA-2 arising from the TFB in the blends decays much faster than the TFB alone sample. The faster PIA decay observed in the blends implies that energy was transferred from the TFB to the acceptor. Furthermore, as shown in Fig. 3(f), after a few picoseconds, the spectral signatures of the PeNCs became more prominent in the blend films without any TFB signature.

Collectively, these observations imply that energy transfer from the donor to the acceptor occurs in the initial 10 ps. The kinetics of the donor and the blends (1 : 3, 1 : 5, and 1 : 8) at PIA-2 are shown in Fig. S1.† The data reveal that the carriers in the pristine donor film are long-lived, whereas the carriers in the blends are much shorter. The lifetime parameter obtained for pristine TFB was approximately 45 ps whereas for the blends, the lifetime of the donor was reduced to 10 ps, suggesting that the energy transfer process concluded within the first 10 ps.

Additionally, the vanishing PIA of TFB, faster decay of PIA, and the rise of PeNC bleach in the blends is clear evidence of energy transfer from TFB to PeNCs. Table 1 shows the lifetime values of the pristine TFB (donor) and the lifetime of the donor in the presence of an acceptor (PeNCs) for different blend ratios. To assess the efficiency of the energy-transfer process, we determined the FRET rate, and FRET efficiency, from the donor lifetimes in the pristine and blended films according to:[39]

$$k_{\mathrm{FRET}} = \frac{1}{\tau_{\mathrm{DA}}} - \frac{1}{\tau_{\mathrm{D}}} \text{ and } E_{\mathrm{FRET}} = 1 - \frac{\tau_{\mathrm{DA}}}{\tau_{\mathrm{D}}}$$

where τ_{DA} is the exciton lifetime of the donor in the presence of the acceptor and τ_{D} is the lifetime of the donor alone. For our donor–acceptor system, we obtain maximum FRET rate of 0.18 ps^{-1} corresponding to the (CBP + TFB) : PeNCs = 1 : 5 blend film and corresponding FRET efficiency of 88.89%. We see that both k_{FRET} and E_{FRET} show an increment in the values from the 1 : 3 blend ratio to the 1 : 5 blend ratio, in accordance with the PL energy-transfer data (Fig. 2a). However, unlike the PL data, we observed a reduction in the FRET rate and FRET efficiency in the 1 : 8 blend film compared with the 1 : 5 blend film. A possible reason for the acceptor PL enhancement in the 1 : 8 blend film could be the reabsorption and the re-emission effects of the acceptor, and not the effective energy transfer from the donor. The observed increase in donor lifetime could then be ascribed to the decrease of the direct energy transfer from donor molecules because of the acceptor behaving more as an independent emitter in its aggregated or unaggregated states.

After studying the photophysical properties of the ternary blend of CBP, TFB, and PeNCs as an efficient donor–acceptor system, it can be concluded that the blend can be used as an emissive material for light-emitting diodes. Most high-performance inverted-architecture PeLEDs have been reported with the device structure of ITO/ZnO/Perovskite/TFB/MoO_3/Au.[40] The hole-conducting TFB has a high hole mobility and a balanced carrier injection speed with ZnO. However, the highest occupied molecular orbital (HOMO) level of TFB (−5.3 eV)[35] is not deep enough to prevent exciton quenching at the TFB–PeNCS interface (valence band maxima, −5.4 eV).[41] Molecular doping is an efficient strategy for lowering the onset voltage of electroluminescence (EL) and improving external

Table 1 Kinetic decay parameters obtained from TAS data at PIA-2, excited at 400 nm

Sample	τ_1 (ps)	τ_2 (ps)	k_{FRET} (ps^{-1})	E_{FRET} (%)
TFB	2 ± 0.25	45 ± 1.04	—	—
(CBP + TFB) : PeNCs (1 : 3)	0.8 ± 0.34	9 ± 1.79	0.09	80.00
(CBP + TFB) : PeNCs (1 : 5)	0.56 ± 0.04	5 ± 0.29	0.18	88.89
(CBP + TFB) : PeNCs (1 : 8)	0.65 ± 0.04	8.7 ± 0.94	0.09	80.67

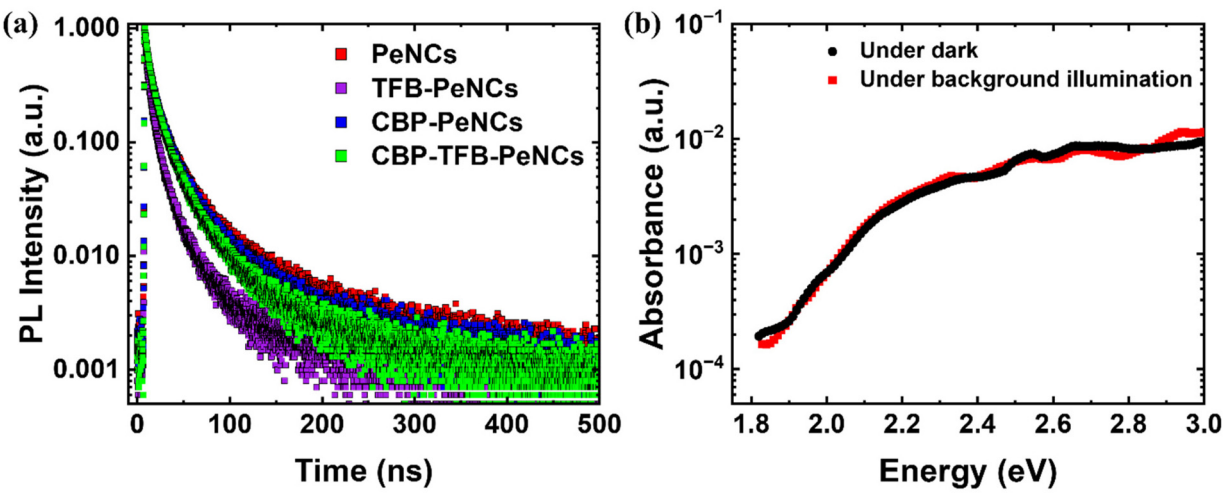

Fig. 4 (a) Lifetime measurements of PeNCs, PeNCs in TFB, PeNCs in CBP, PeNCs in CBP and TFB, and (b) Photothermal deflection spectroscopy of the CBP–TFB–PeNCs blend film under dark and background illumination conditions showing photo stability of the blend.

Table 2 PL decay lifetimes obtained from TCSPC, excited at 375 nm

Sample	τ_1 (ns)	τ_2 (ns)
PeNCs	4.48 ± 0.02	24.22 ± 0.12
TFB–PeNCs	2.37 ± 0.01	12.29 ± 0.05
CBP–PeNCs	4.61 ± 0.02	22.75 ± 0.11
CBP–TFB–PeNCs	4.22 ± 0.02	20.45 ± 0.09

quantum efficiency (EQE) because of the better injection of carriers.[42] Doping a hole conducting molecule (CBP) with TFB can eliminate interface exciton quenching due to its lower HOMO level (6.1 eV)[35] and can help achieve cascade charge transfer during device EL experiments. Therefore, we mixed both CBP and TFB with the PeNCs to obtain a highly emissive blend that can be used as an active layer for PeLEDs. Based on these observations, we propose an architecture (Fig. S3a†) for the fabrication of PeLEDs with a blend of CBP, TFB, and PeNCs as an emissive layer. The corresponding flat-band energy level diagram is shown in Fig. S3b.† This blend holds the promise of providing the dual benefits of cascade energy and charge transfer to simultaneously achieve improved recombination, reduced exciton quenching, and high EQEs.

We employed a time-correlated single-photon counting (TCSPC) setup to investigate the PL decay and corresponding lifetimes of the PeNCs in the pristine, CBP–PeNC, TFB–PeNC, and CBP–TFB–PeNC films (Fig. 4a) to probe the quenching effect of the TFB–PeNC interface. The fitting curves are shown in Fig. S2.† The obtained lifetime data are listed in Table 2. Exciton lifetime measurements provide evidence that the doping of TFB and CBP effectively reduces the TFB–PeNC interfacial exciton quenching. Photothermal deflection spectroscopy (PDS) was employed to assess the photostability of the CBP–TFB–PeNCs blend film. The absorption spectra (Fig. 4b) remained unchanged under both dark and background illumination conditions, indicating the optical stability of the blend.

Conclusions

In conclusion, we present the first demonstration of Förster Resonance Energy Transfer between a polymer matrix and perovskite nanocrystals in a donor–acceptor system to achieve enhanced pure-red emission. TFB, a hole-transporting polymer, was employed as the donor, whereas methylammonium-based lead mixed-halide red-emitting PeNCs served as the acceptor. Thin films with varying donor-to-acceptor ratios were fabricated, showing a decrease in the donor PL intensity and a corresponding increase in the acceptor PL intensity as the acceptor concentration increased. Femtosecond transient absorption spectroscopy further revealed a reduction in the donor lifetime with acceptor addition, confirming the FRET mechanism. The FRET rate and efficiency were calculated to be 0.18 ps^{-1} and 88.89%, demonstrating the high energy-transfer efficiency of this system. Additionally, the inclusion of CBP in the blend mitigates exciton quenching at the TFB–PeNC interface and facilitated the cascade charge transfer. This can lead to enhanced recombination efficiencies and reduced turn-on voltages for fabrication of efficient pure-red PeLEDs and inspire work on other colours of PeLEDs.

Author contributions

JS and AS conceptualised the idea and experiments. AS and AAAK contributed to the initial methodology development for the red PeNC synthesis. JS performed the optimization and synthesis of the red PeNC in supervision of AS and AAAK. JS performed all the sample preparation and spectroscopy experiments other than fs-TAS. RM, VRS and SSKR performed the fs-TAS experiments and data analysis in assistance of AS and JS. AR performed the PDS measurements and analysis. All the authors contributed to the writing of this manuscript.

Data availability

The data supporting this article have been included as part of the ESI.†

Conflicts of interest

There are no conflicts to declare.

Acknowledgements

We express our gratitude to DST, SERB, MoE (MHRD), MeitY, QURP (Government of Karnataka) and the Pratiksha Trust for their generous funding and support for this research. We extend our thanks to the Micro & Nano Characterization Facility (MNCF) at CeNSE for providing access to advanced characterization facilities. We are also deeply grateful to Dr Gopa Sardar for her invaluable suggestions and guidance throughout the course of this study. R. S. S. K. thanks Prof. S. Venugopal Rao, University of Hyderabad for providing access to the femtosecond laser facility. Funding support by DAE-BRNS (58/14/06/2023-BRNS/37030) is acknowledged. R. M. acknowledges the funding support from PMRF. A. S. and A. A. A. K. would like to thank the generous funding support from the Distinguished Scientist Fellowship Program (DSFP) by King Saud University, Riyadh, Saudi Arabia.

References

1 J. Hu, C. Bi, K. Ren, X. Zhang, W. Wang, S. Ma, M. Wei, Y. Lu and M. Sui, *Nano Lett.*, 2024, **24**, 4571–4579.
2 M. Jiang, Z. Hu, L. K. Ono and Y. Qi, *Nano Res.*, 2021, **14**, 191–197.
3 Z. K. Tan, R. S. Moghaddam, M. L. Lai, P. Docampo, R. Higler, F. Deschler, M. Price, A. Sadhanala, L. M. Pazos, D. Credgington, F. Hanusch, T. Bein, H. J. Snaith and R. H. Friend, *Nat. Nanotechnol.*, 2014, **9**, 687–692.

4 D. Chen, P. K. Ko, C. H. A. Li, B. Zou, P. Geng, L. Guo and J. E. Halpert, *ACS Energy Lett.*, 2023, **8**, 410–416.
5 J. S. Yao, J. Ge, K. H. Wang, G. Zhang, B. S. Zhu, C. Chen, Q. Zhang, Y. Luo, S. H. Yu and H. B. Yao, *J. Am. Chem. Soc.*, 2019, **141**, 2069–2079.
6 L. Protesescu, S. Yakunin, M. I. Bodnarchuk, F. Krieg, R. Caputo, C. H. Hendon, R. X. Yang, A. Walsh and M. V. Kovalenko, *Nano Lett.*, 2015, **15**, 3692–3696.
7 M. Xie, J. Guo, X. Zhang, C. Bi, L. Zhang, Z. Chu, W. Zheng, J. You and J. Tian, *Nano Lett.*, 2022, **22**, 8266–8273.
8 S. Wang, Q. Zhao, A. Hazarika, S. Li, Y. Wu, Y. Zhai, X. Chen, J. M. Luther and G. Li, *Nat. Commun.*, 2023, **14**, 1–12.
9 H. S. Yang, E. H. Suh, S. H. Noh, J. Jung, J. G. Oh, K. H. Lee, D. Lee and J. Jang, *Chem. Eng. J.*, 2023, **454**, 140331.
10 S. Liu, H. Zhan, C. Qin and C. Qin, *J. Phys. Chem. Lett.*, 2023, **14**, 73–79.
11 L. Kong, X. Zhang, Y. Li, H. Wang, Y. Jiang, S. Wang, M. You, C. Zhang, T. Zhang, S. V. Kershaw, W. Zheng, Y. Yang, Q. Lin, M. Yuan, A. L. Rogach and X. Yang, *Nat. Commun.*, 2021, **12**, 1–8.
12 L. Zhang, C. Sun, T. He, Y. Jiang, J. Wei, Y. Huang and M. Yuan, *Light: Sci. Appl.*, 2021, **10**, 1–26.
13 K. Wang, Z. Y. Lin, Z. Zhang, L. Jin, K. Ma, A. H. Coffey, H. R. Atapattu, Y. Gao, J. Y. Park, Z. Wei, B. P. Finkenauer, C. Zhu, X. Meng, S. N. Chowdhury, Z. Chen, T. Terlier, T. H. Do, Y. Yao, K. R. Graham, A. Boltasseva, T. F. Guo, L. Huang, H. Gao, B. M. Savoie and L. Dou, *Nat. Commun.*, 2023, **14**, 1–11.
14 L. Yang, Y. Zhang, J. Ma, P. Chen, Y. Yu, M. Shao, Y. Yu and M. Shao, *ACS Energy Lett.*, 2021, **6**, 2386–2394.
15 J. Zhang, B. Cai, X. Zhou, F. Yuan, C. Yin, H. Wang, H. Chen, X. Ji, X. Liang, C. Shen, Y. Wang, Z. Ma, J. Qing, Z. Shi, Z. Hu, L. Hou, H. Zeng, S. Bai and F. Gao, *Adv. Mater.*, 2023, **35**, 2303938.
16 Y. Hassan, J. H. Park, M. L. Crawford, A. Sadhanala, J. Lee, J. C. Sadighian, E. Mosconi, R. Shivanna, E. Radicchi, M. Jeong, C. Yang, H. Choi, S. H. Park, M. H. Song, F. De Angelis, C. Y. Wong, R. H. Friend, B. R. Lee and H. J. Snaith, *Nature*, 2021, **591**(7848), 72–77.
17 T. Chiba, Y. Hayashi, H. Ebe, K. Hoshi, J. Sato, S. Sato, Y. J. Pu, S. Ohisa and J. Kido, *Nat. Photonics*, 2018, **12**, 681–687.
18 J. C. Yu, A. Y. Lee, D. B. Kim, E. D. Jung, D. W. Kim and M. H. Song, *Adv. Mater. Technol.*, 2017, **2**, 1700003.
19 M. A. Sandzhieva, L. E. Zelenkov, L. A. Otpushchennikov, S. Miltsov, E. V. Zhukova, L. S. Litvinova, S. A. Cherevkov, I. M. Sevastianova, D. Shestakov, A. V. Yakimansky and S. V. Makarov, *Photonics Nanostruct.*, 2024, **58**, 101239.
20 G. Li, Z. K. Tan, D. Di, M. L. Lai, L. Jiang, J. H. W. Lim, R. H. Friend and N. C. Greenham, *Nano Lett.*, 2015, **15**, 2640–2644.
21 M. Berggren, O. Inganäs, G. Gustafsson, J. Rasmusson, M. R. Andersson, T. Hjertberg and O. Wennerström, *Nature*, 1994, **372**(6505), 444–446.
22 P. K. H. Ho, J. I. S. Kim, J. H. Burroughes, H. Becker, S. F. Y. Li, T. M. Brown, F. Cacialli and R. H. Friend, *Nature*, 2000, **404**(6777), 481–484.
23 M. U. Hassaan, Y. C. Liu, K. U. Hasan, M. Rafique, A. K. Yetisen, H. Butt and R. H. Friend, *ACS Photonics*, 2018, **5**, 607–613.
24 B. R. Lee, W. Lee, T. L. Nguyen, J. S. Park, J. S. Kim, J. Y. Kim, H. Y. Woo and M. H. Song, *ACS Appl. Mater. Interfaces*, 2013, **5**, 5690–5695.
25 J. R. Lakowicz, *Principles of Fluorescence Spectroscopy*, 2006, pp. 1–954.
26 T. Virgili, D. G. Lidzey and D. D. C. Bradley, *Adv. Mater.*, 2000, **12**, 58–62.
27 C. W. Tang, S. A. Vanslyke and C. H. Chen, *J. Appl. Phys.*, 1989, **65**, 3610–3616.
28 C. R. McNeill and N. C. Greenham, *Adv. Mater.*, 2009, **21**, 3840–3850.
29 T. Förster, *Discuss. Faraday Soc.*, 1959, **27**, 7–17.
30 I. N. Kang, D. H. Hwang, H. K. Shim, T. Zyung and J. J. Kim, *Macromolecules*, 1996, **29**, 165–169.
31 H. Mattoussi, H. Murata, C. D. Merritt, Y. Iizumi, J. Kido and Z. H. Kafafi, *J. Appl. Phys.*, 1999, **86**, 2642–2650.
32 F. Laquai, Y. S. Park, J. J. Kim and T. Basché, *Macromol. Rapid Commun.*, 2009, **30**, 1203–1231.
33 S. E. Shaheen, B. Kippelen, N. Peyghambarian, J. F. Wang, J. D. Anderson, E. A. Mash, P. A. Lee, N. R. Armstrong and Y. Kawabe, *J. Appl. Phys.*, 1999, **85**, 7939–7945.
34 Y. Zhao, L. Chen, J. Wu, X. Tan, Z. Xiong and Y. Lei, *IEEE Electron Device Lett.*, 2020, **41**, 80–83.
35 T. Zhang, M. Long, L. Pan, K. Ngai, M. Qin, F. Xie, X. Lu, J. Chen and J. Xu, *Sci. Bull.*, 2020, **65**, 1832–1839.
36 N. J. L. K. Davis, F. J. de la Peña, M. Tabachnyk, J. M. Richter, R. D. Lamboll, E. P. Booker, F. W. R. Rivarola, J. T. Griffiths, C. Ducati, S. M. Menke, F. Deschler and N. C. Greenham, *J. Phys. Chem. C*, 2017, **121**, 3790–3796.
37 V. Ravali and T. Ghosh, *Chem. Commun.*, 2023, **59**, 13939–13950.
38 X. Deng, X. Wen, S. Huang, R. Sheng, T. Harada, T. W. Kee, M. Green and A. Ho-Baillie, *J. Phys. Chem. C*, 2016, **120**, 2542–2547.
39 I. Majoul, Y. Jia and R. Duden, *Handbook of Biological Confocal Microscopy*, 3rd edn, 2006, pp. 788–808.
40 N. Wang, L. Cheng, R. Ge, S. Zhang, Y. Miao, W. Zou, C. Yi, Y. Sun, Y. Cao, R. Yang, Y. Wei, Q. Guo, Y. Ke, M. Yu, Y. Jin, Y. Liu, Q. Ding, D. Di, L. Yang, G. Xing, H. Tian, C. Jin, F. Gao, R. H. Friend, J. Wang and W. Huang, *Nat. Photonics*, 2016, **10**(11), 699–704.
41 Y. Hassan, O. J. Ashton, J. H. Park, G. Li, N. Sakai, B. Wenger, A. A. Haghighirad, N. K. Noel, M. H. Song, B. R. Lee, R. H. Friend and H. J. Snaith, *J. Am. Chem. Soc.*, 2019, **141**, 1269–1279.
42 J. Blochwitz, M. Pfeiffer, T. Fritz and K. Leo, *Appl. Phys. Lett.*, 1998, **73**, 729–731.